31st Annual International Conference of the IEEE EMBS
Minneapolis, Minnesota, USA, September 2-6, 2009

Detection of the Temporal Arcade in Fundus Images of the Retina Using the Hough Transform

Faraz Oloumi and Rangaraj M. Rangayyan*
Department of Electrical and Computer Engineering, Schulich School of Engineering, University of Calgary
2500 University Drive NW, Calgary, Alberta, Canada, T2N 1N4 *ranga@ucalgary.ca

Abstract— **Quantitative analysis of the vascular architecture of the retina can help in monitoring the effects of retinopathy on the visual system. Retinopathy affects the blood vessels in the retina through modification of the shape, width, tortuosity, and the angle of insertion of the temporal arcade. Monitoring the openness of the temporal arcade and changes with treatment can facilitate improved diagnosis and optimized treatment. We propose methods for the detection and parametric modeling of the temporal arcade, including gradient operators and Gabor functions to detect retinal vessels, and the Hough transform to detect parabolic forms. Results obtained with 40 images of the retina indicate accurate to acceptable results for 24 images and partial fits of the parabolic models for 11 images.**

I. Introduction

A. Retinopathy

Diabetes, hypertension, arteriosclerosis, and retinopathy of prematurity (ROP) affect the structure of the blood vessels in the retina by modifying their width, shape, and tortuosity [1], [2], [3]. Some of the degenerating conditions of ROP associated with posterior changes are straightening of the blood vessels in the temporal arcade and a decrease in the angle of insertion of the temporal arcade [4]. The recognition of low levels of tortuosity and dilation is difficult for even expert observers, as indicated by Freedman et al. [5]. Whereas changes in tortuosity have been observed to be consistent with the severity of the disease [6], [1], quantifying changes to the width of the vessels can be difficult due to the fact that such changes are comparable to the resolution of the image [2]. Furthermore, changes to the width may not be consistent with the severity of the disease [7]. These factors justify the need for a simple and reliable system for early detection of changes in fundus images of the retina leading to pre-plus and plus disease, and ultimately ROP, in the form of a semi-automated or automated computer program. Because the diseases mentioned above change the angle of insertion of the temporal arcade, the openness or aperture of the main temporal arcade also changes. Consequently, the detection of the main temporal arcade and quantitative analysis of its openness could help in diagnosing and monitoring the stages of retinopathy, as well as determining the effects of therapy.

B. Detection of the Temporal Arcade

The detection of the temporal arcade can help in the localization of other features of the retina, such as the optic nerve head (ONH) and fovea [8], [9], [10], [11]. The temporal arcade, by itself, does not appear to have been used for quantitative analysis of retinal vasculature. By simple examination of retinal images, it can be seen that the temporal arcade originates from the ONH and expands in a parabolic pattern. The parabolic profile can be used to derive an estimate of the openness of the temporal arcade.

Foracchia et al. [11] proposed a method for the detection of the ONH by defining a directional model for the vessels, assuming that the main vessels originate from the ONH and extend in paths that can be geometrically modeled as parabolas. A directional model was defined using the parabolic formulation and assuming that the preferred direction of the vessels is tangential to the parabolas themselves. With the model and data indicating the center points, direction, and caliber of the vessels, by using a residual sum of squares method, the parameters of the model were identified.

Using an estimate of the ONH location and a binarized image of the vasculature, Tobin et al. [9] proposed to apply a parabolic model to the statistical distribution of a set of points given by a morphologically skeletonized vascular image to find an estimate of the retinal raphe. A parabola of the form $ay^2 = |x|$ was modified to accommodate for the shifted vertex at the most likely ONH location and the angle of rotation of the retinal raphe, β. The resulting model and the skeletonized image were used with Marquardt's least-squares method to estimate the parameters a and β.

Using an active shape model (ASM) and defining a point distribution model (PDM), Li and Chutatape [10] proposed a method to detect the boundary of the ONH and the main course of the blood vessels. Using ASM and principal component analysis, the location of the ONH was estimated. A modified ASM was used to extract the main course of the blood vessels. Thirty landmark points on the main course of the vessels were used to derive the PDM. The Hough transform and linear least-squares fitting methods were combined to estimate a parabolic model. The rotation variable was allowed to vary from $+45°$ to $-45°$ and the vertex coordinate was approximated at half of the radius of the ONH nasal to the ONH so that only the variable a, the aperture of the parabola, needed to be estimated.

Fleming et al. [8] proposed a method to extract the temporal arcade by means of vessel enhancement and semi-elliptical curve fitting using the generalized Hough transform (GHT). First, the vessels were enhanced to get a magnitude image and a phase image of the vascular architecture. As-

This work was supported by the Natural Sciences and Engineering Research Council of Canada. We thank Xiaolu Zhu and Dr. Anna Ells for their contributions to this work.

suming that, having an edge map and knowing the orientation of the arcade, a reference point can only be at one of a few locations, the GHT was applied to a skeletonized image of the vasculature. The Hough space dimension was set to be five, with variables for inclination, horizontal axis length, left or right opening, and the location of the center of the ellipse. Anatomical restrictions were applied to the variables to limit the number of semi-ellipses generated by the method. The global maximum in the Hough space was selected to derive the closest fit to the temporal arcade.

Because the temporal arcade can be geometrically modeled as a parabola, we propose a form of the GHT that can be used to detect the temporal arcade in a retinal fundus image.

II. Methods

A. Preprocessing of Images

The proposed methods were tested with fundus images of the retina from the Digital Retinal Images for Vessel Extraction [12] (DRIVE) database, which contains 40 images. Each image is of size 584×565 pixels, with a field of view of 45° and a spatial resolution of 20 μm per pixel. After converting each pixel in a given image to a vector of color components and normalizing each component (dividing by 255), the result was converted to the luminance component Y, computed as $Y = 0.299R + 0.587G + 0.114B$, where R, G, and B are the red, green, and blue components, respectively, of the color image. The effective region of the image was obtained by thresholding the luminance image with a normalized threshold of 0.1. Artifacts present at the edges were removed by applying morphological erosion with a disk-shaped structuring element of diameter 10 pixels. In order to avoid detection of the edges of the effective region, the resulting image was extended beyond the limits of its effective region as follows [13]: First, a four-pixel neighborhood was used to identify the pixels at the outer edge of the effective region. For each of the pixels identified, the mean gray level was computed over all pixels in a 21×21 neighborhood that were also within the effective region. The mean value was assigned to the corresponding pixel location in the gray-scale image. The effective region was merged with the outer edge pixels, forming an extended effective region. The procedure was repeated 50 times, extending the image by a ribbon of width 50 pixels.

B. Derivation of an Edge Map of the Retinal Vessels

The Sobel edge detector [14], [15] was used as one option for the detection of retinal vessels. The Sobel operators for the horizontal and vertical gradients, respectively, are

$$\begin{bmatrix} -1 & -2 & -1 \\ 0 & 0 & 0 \\ 1 & 2 & 1 \end{bmatrix}, \begin{bmatrix} -1 & 0 & 1 \\ -2 & 0 & 2 \\ -1 & 0 & 1 \end{bmatrix}. \quad (1)$$

The combined gradient magnitude was obtained as $G(x,y) = [G_x^2(x,y) + G_y^2(x,y)]^{\frac{1}{2}}$, where $G_x(x,y)$ and $G_y(x,y)$ are the horizontal and vertical components of the gradient, respectively. An automatic threshold, provided by the Sobel edge detection function in Matlab [16], was applied to the gradient magnitude image to obtain a binary edge map.

As a second option to obtain a map of the retinal vessels, the Gabor filter [13] was used. The Gabor filter is defined by the standard deviation values of a Gaussian in the x and y directions (σ_x and σ_y) and the frequency f_o of the modulating sinusoid as [17]

$$g(x,y) = \frac{1}{2\pi\sigma_x\sigma_y} \exp\left[-\frac{1}{2}\left(\frac{x^2}{\sigma_x^2} + \frac{y^2}{\sigma_y^2}\right)\right] \cos(2\pi f_o x). \quad (2)$$

The value of σ_x was defined in relation to the average thickness of the vessels to be detected, τ, as $\sigma_x = \tau/\{2\sqrt{2\ln 2}\}$. The value of f_o was defined as $f_o = 1/\tau$. The parameter σ_y was set as $\sigma_y = 2\,\sigma_x$. A bank of 180 filters was created by rotation of the basic Gabor filter specified above to span the range $[-90^\circ, 90^\circ]$ in steps of 1°. A magnitude response image was created by using the maximum value of the responses of the 180 Gabor filters for each pixel. Only one scale of $\tau = 16$ pixels was used to emphasize the major blood vessels, i.e., the temporal arcade. The magnitude image was thresholded to obtain a binary image of the blood vessels in two ways: *(a)* Otsu's [18] method for optimal thresholding; *(b)* Fixed thresholding by setting a fixed threshold of 0.01 of the normalized intensity.

After getting the binary image of vessels, the morphological processes of skeletonization [14] and area open [19] were applied to get a skeletonized image of the blood vessels, as well as to clean the image by eliminating isolated pixels and short line segments related to small blood vessels. The skeletonization procedure uses a form of the erosion process and leaves only lines of single-pixel thickness without altering the structure of the objects. The structuring element used was a disk of radius 3 pixels. The area open procedure detects any segment of connected pixels having a specified maximum number of pixels and removes them. The area open procedure was also applied to the Sobel edge image to eliminate small artifacts.

C. Hough Transform for the Detection of Parabolas

Hough [20] proposed a method for the detection of straight lines in images. The Hough transform can be modified to detect parametric curves such as circles and parabolas [15], [21], [22], [23]. The general formula defining a parabola with its directrix parallel to the y-axis and its symmetrical axis parallel to the x-axis is

$$(y - y_o)^2 = 4a(x - x_o), \quad (3)$$

where (x_o, y_o) is the vertex of the parabola and the quantity $4a$ is known as the latus rectum. The value of a governs the aperture of the parabola and indicates the direction of the opening of the parabola; for a positive a value, the parabola opens to the right. The parameters (x_o, y_o, a) define the parameter space or the Hough space, represented by an accumulator, A. For every non-zero pixel in the image domain there exists a parabola in the Hough space for each value of a; a single point in the Hough space defines a

parabola in the image domain. The size of each (x_o, y_o) plane in the Hough space was defined to be the same as the size of the image (584×565 pixels). The value of a is restricted by physiological limits on the arcade and the size of the image. For the DRIVE database [12], the value of a was translated to the range $[25, 60]$. In order not to make the accumulator too large, only positive values of a were defined. If an image had the temporal arcade opening to the left, it was rotated by $180°$ so the arcade would open to the right in the data used for the subsequent steps. For each non-zero pixel in the given edge map, the parameter a was computed for each (x_o, y_o) in the parameter space, and the corresponding accumulator cell was incremented if the value of a was within the specified range. The point in the Hough space with the highest value was selected to obtain the parameters (x_o, y_o, a) of the best-fitting parabolic model of the temporal arcade.

III. Results

The original version of image 14 from the DRIVE database is shown in Fig. 1 (a). The preprocessed gray-scale image is shown in Fig. 1 (b). The binary edge image of the blood vessels obtained using the Sobel edge operator is shown in Fig. 1 (c). The magnitude response of the Gabor filters is shown in Fig. 1 (d). The magnitude response was thresholded to get a binary image of the blood vessels, expected to contain the temporal arcade and not the minor vessels because of the large value of $\tau = 16$ used. The skeletonized image, obtained from the thresholded image, is shown in Fig. 1 (e). The skeletonized image was cleaned using the area open procedure; the result is shown in Fig. 1 (f). The vessel maps obtained from the Sobel and Gabor approaches were analyzed using the Hough transform. The Hough space plane for $a = -60$ is shown in Fig. 1 (g), which contains the global maximum in this case. The parabola with the detected vertex coordinates and the value of a was drawn on the original image; the result is shown in Fig. 1 (h). The results of parabolic fitting using the fixed thresholding method applied to the results of Gabor filtering of the 40 images of the DRIVE database indicated three accurate fits, 21 acceptable fits, 11 partial fits, and five unacceptable fits. An accurate fit is indicated by a parabola that fits at least 90% of the temporal arcade and has its vertex in, or close to, the ONH, as shown in Fig. 2 (a). An acceptable fit indicates cases where more than 50% of the arcade is fitted by the parabola, as in the case shown in Fig. 2 (b). Cases where one part of the arcade agrees with the parabolic model, but the rest does not, either due to a non-parabolic form of the arcade or due to the model being attracted by other blood vessels, are termed as partial fits; an example is shown in Fig. 2 (c). Images with unacceptable results were found to be non-standard images that are not macula centered [24], as shown in Fig. 2 (d).

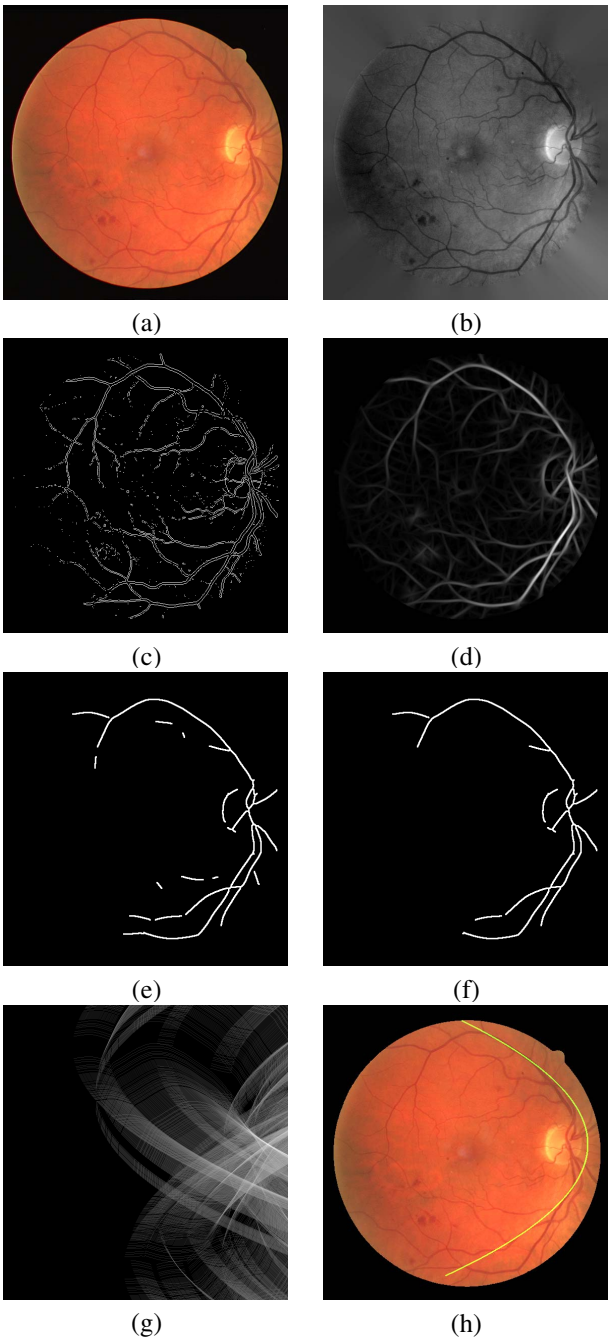

Fig. 1. (a) Image 14 of the DRIVE database (565×584 pixels). (b) The preprocessed gray-scale image. (c) Result of edge detection using the Sobel operators. (d) The Gabor magnitude response. (e) Skeletonized image obtained from the result in (d). (f) The cleaned skeletonized image using the area open procedure. (g) The Hough space for $a = -60$ including the global maximum. (h) The original image with the best-fitting parabola.

IV. Discussion and Future Work

The fixed thresholding method applied to the Gabor magnitude response led to better results than automatic thresholding of the same and the results of the Sobel edge operators. The automatic thresholding procedure did not remove the minor blood vessels to the same extent as the fixed thresholding method. The skeletonized image obtained from the result of fixed thresholding mostly contained the main course of the blood vessels, i.e., the temporal arcade, and is suitable for analysis in the Hough space. The Sobel edge detector led to the representation of multiple parabolas

in the Hough space because thick blood vessels have double edges in the resulting binary image. A center-line or skeleton image is better suited for analysis using the Hough transform than an image with multiple edges for the object of interest. Furthermore, because the temporal arcade does not always follow a perfect parabolic path, the results of the Hough transform may provide only a partial fit or an acceptable fit in several cases. Small vessels left after thresholding may affect the result of the Hough transform, especially if they form parabolic patterns themselves.

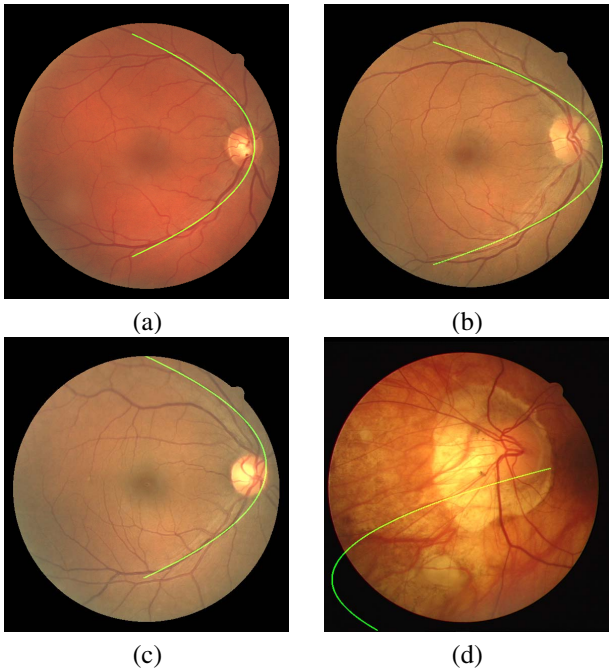

Fig. 2. Examples of (a) an accurately fitted parabola, (b) an acceptable fit, (c) a partially fitted parabola, and (d) an unacceptable fit.

Although the proposed methods have shown promising potential, there are limitations that need to be addressed. The Hough transform procedure developed in the present work does not take into account any rotation that might exist between the horizontal axis of the image and the retinal raphe; this step will be incorporated in future works. Prior knowledge of the location of the ONH, and hence the point of convergence of the temporal arcade, could assist in delimiting the range of search for the vertex of the parabolic model. An algorithm to detect and analyze several local maxima in the Hough space may lead to better results, because the global maximum may not always provide the best-fitting parabola. The results need to be evaluated by an expert: further work will include objective comparison of the parabolic model with the temporal arcade marked by an ophthalmologist.

V. Conclusion

The proposed methods have shown good results in the detection of the temporal arcade in fundus images of the retina. With further improvements in the accuracy of the models derived, the methods should lead to improved diagnosis and therapy of retinopathy.

References

[1] Heneghan C, Flynn J, O'Keefe M, and Cahill M, "Characterization of changes in blood vessels width and tortuosity in retinopathy of prematurity using image analysis," *Medical Image Analysis*, vol. 6, no. 1, pp. 407–429, 2002.

[2] Wilson CM, Cocker KD, Moseley MJ, Paterson C, Clay ST, Schulenburg WE, Mills MD, Ells AL, Parker KH, Quinn GE, Fielder AR, and Ng J, "Computerized analysis of retinal vessel width and tortuosity in premature infants," *Investigative Ophthalmology and Visual Science*, vol. 49, no. 1, pp. 3577–3585, 2008.

[3] Patton N, Aslam TM, MacGillivray T, Deary IJ, Dhillon B, Eikelboom RH, Yogesan K, and Constable IJ, "Retinal image analysis: Concepts, applications and potential," *Progress in Retinal and Eye Research*, vol. 25, no. 1, pp. 99–127, 2006.

[4] International Committee for the Classification of Retinopathy of Prematurity, "The international classification of retinopathy of prematurity revisited," *Archives of Ophthalmology*, vol. 123, pp. 991–999, 2005.

[5] Freedman SF, Kylstra JA, Hall JG, and Capowski JJ, "Plus disease in retinopathy of prematurity - Photographic evaluation by an expert panel," *Investigative Ophthalmology and Visual Science*, , no. 1, pp. 36–76, 1995.

[6] Hart WE, Goldbaum M, Côté B, Kube P, and Nelson MR, "Measurement and classification of retinal vascular tortuosity," *International Journal of Medical Informatics*, vol. 53, no. 2-3, pp. 239–252, 1999.

[7] Swanson C, Cocker KD, Parker KH, Moseley MJ, and Fielder AR, "Semiautomated computer analysis of vessel growth in preterm infants without and with ROP," *British Journal of Ophthalmology*, vol. 87, no. 12, pp. 1474–1477, 2003.

[8] Fleming AD, Goatman KA, Philip S, Olson JA, and Sharp PF, "Automatic detection of retinal anatomy to assist diabetic retinopathy screening," *Physics in Medicine and Biology*, vol. 52, pp. 331–345, 2007.

[9] Tobin KW, Chaum E, Govindasamy VP, and Karnowski TP, "Detection of anatomic structures in human retinal imagery," *IEEE Transactions on Medical Imaging*, vol. 26, no. 12, pp. 1729–1739, December 2007.

[10] Li H and Chutatape O, "Automated feature extraction in color retinal images by a model based approach," *IEEE Transactions on Biomedical Engineering*, vol. 51, no. 2, pp. 246–254, 2004.

[11] Foracchia M, Grisan E, and Ruggeri A, "Detection of optic disc in retinal images by means of a geometrical model of vessel structure," *IEEE Transactions on Medical Imaging*, vol. 23, no. 10, pp. 1189–1195, 2004.

[12] DRIVE: Digital Retinal Images for Vessel Extraction, http:// www. isi.uu.nl/ Research/ Databases/ DRIVE/, accessed on March 24, 2009.

[13] Rangayyan RM, Ayres FJ, Oloumi F, Oloumi F, and Eshghzadeh-Zanjani P, "Detection of blood vessels in the retina with multiscale Gabor filters," *Journal of Electronic Imaging*, vol. 17, pp. 023018:1–7, April-June 2008.

[14] Gonzalez RC and Woods RE, *Digital Image Processing*, Prentice Hall, Upper Saddle River, NJ, 2nd edition, 2002.

[15] Rangayyan RM, *Biomedical Image Analysis*, CRC, Boca Raton, FL, 2005.

[16] The MathWorks, http:// www. mathworks. com/, accessed on March 24, 2009.

[17] Ayres FJ and Rangayyan RM, "Design and performance analysis of oriented feature detectors," *Journal of Electronic Imaging*, vol. 16, no. 2, pp. 023007:1–12, 2007.

[18] Otsu N, "A threshold selection method from gray-level histograms," *Automatica*, vol. 11, pp. 285–296, 1975.

[19] Acton ST, "A pyramidal algorithm for area morphology," in *Proceedings of IEEE International Conference on Image Processing*, Vancouver, BC, Canada, 2000, pp. 10–13.

[20] Hough PVC, "Method and means for recognizing complex patterns," US Patent 3, 069, 654, December 18, 1962.

[21] Jafri MZM and Deravi F, "Efficient algorithm for the detection of parabolic curves," *Vision Geometry III*, vol. 2356, pp. 53–62, 1994.

[22] Ballard DH, "Generalizing the Hough transform to detect arbitrary shapes," *Pattern Recognition*, vol. 13, no. 2, pp. 111–122, 1981.

[23] Wechsler H and Sklansky J, "Finding the rib cage in chest radiographs," *Pattern Recognition*, vol. 9, no. 1, pp. 21–30, 1977.

[24] Fleming AD, Philip S, Goatman KA, Olson JA, and Sharp PF, "Automated assessment of diabetic retinal image quality based on clarity and field definition," *Investigative Ophthalmology & Visual Science*, vol. 47, no. 3, pp. 1120–1125, 2006.